

01 Feb 2015

Investigating the Solubility and Cytocompatibility of CaO-Na₂O-SiO₂/TiO₂ Bioactive Glasses

Anthony W. Wren


Aisling Coughlan

Courtney M. Smith

Sarah P. Hudson

et. al. For a complete list of authors, see https://scholarsmine.mst.edu/che_bioeng_facwork/1129

Follow this and additional works at: https://scholarsmine.mst.edu/che_bioeng_facwork

 Part of the [Biochemical and Biomolecular Engineering Commons](#), and the [Biomedical Devices and Instrumentation Commons](#)

Recommended Citation

A. W. Wren et al., "Investigating the Solubility and Cytocompatibility of CaO-Na₂O-SiO₂/TiO₂ Bioactive Glasses," *Journal of Biomedical Materials Research - Part A*, vol. 103, no. 2, pp. 709 - 720, Wiley, Feb 2015. The definitive version is available at <https://doi.org/10.1002/jbm.a.35223>

This Article - Journal is brought to you for free and open access by Scholars' Mine. It has been accepted for inclusion in Chemical and Biochemical Engineering Faculty Research & Creative Works by an authorized administrator of Scholars' Mine. This work is protected by U. S. Copyright Law. Unauthorized use including reproduction for redistribution requires the permission of the copyright holder. For more information, please contact scholarsmine@mst.edu.

Investigating the solubility and cytocompatibility of CaO–Na₂O–SiO₂/TiO₂ bioactive glasses

Anthony W. Wren,¹ Aisling Coughlan,² Courtney M. Smith,¹ Sarah P. Hudson,³ Fathima R. Laffir,³ Mark R. Towler⁴

¹Inamori School of Engineering, Alfred University, Alfred, New York

²School of Materials Engineering, Purdue University, West Lafayette, Indiana

³Materials and Surface Science Institute, University of Limerick, Limerick, Ireland

⁴Department of Mechanical and Industrial Engineering, Ryerson University, Toronto, Canada

Received 28 April 2014; accepted 6 May 2014

Published online 22 May 2014 in Wiley Online Library (wileyonlinelibrary.com). DOI: 10.1002/jbm.a.35223

Abstract: This study aims to investigate the solubility of a series of titanium (TiO₂)-containing bioactive glasses and their subsequent effect on cell viability. Five glasses were synthesized in the composition range SiO₂–Na₂O–CaO with 5 mol % of increments TiO₂ substituted for SiO₂. Glass solubility was investigated with respect to (1) exposed surface area, (2) particle size, (3) incubation time, and (4) compositional effects. Ion release profiles showed that sodium (Na⁺) presented high release rates after 1 day and were unchanged between 7 and 14 days. Calcium (Ca²⁺) release presented a significant change at each time period and was also composi-

tion dependent, where a reduction in Ca²⁺ release is observed with an increase in TiO₂ concentration. Silica (Si⁴⁺) release did not present any clear trends while no titanium (Ti⁴⁺) was released. Cell numbers were found to increase up to 44%, compared to the growing control population, with a reduction in particle size and with the inclusion of TiO₂ in the glass composition. © 2014 Wiley Periodicals, Inc. *J Biomed Mater Res Part A*: 103A: 709–720, 2015.

Key Words: bioactive glass, solubility, particle size, ion release, cell culture

How to cite this article: Wren AW, Coughlan A, Smith CM, Hudson SP, Laffir FR, Towler MR. 2015. Investigating the solubility and cytocompatibility of CaO–Na₂O–SiO₂/TiO₂ bioactive glasses. *J Biomed Mater Res Part A* 2015;103A:709–720.

INTRODUCTION

Bioactive glasses are a class of materials that were conceived in the late 1960s by Prof. L. Hench at the University of Florida. Bioactive glasses have been used to develop numerous materials such as glass–ceramic scaffolds for orthopedic applications^{1–3}; glass polyalkenoate cements as bone adhesives^{4–6} and glass microspheres for cancer treatment.^{7–9} However, since their inception bioactive glasses have been utilized primarily for skeletal augmentation or repair^{10–12} as they stimulate osteogenesis in *in vitro* models.^{11,12} The most widely known bioactive glass, 45S5 Bioglass (Na₂O–CaO–SiO₂–P₂O₅), sees applications predominantly in orthopedics as a bone void filler. Early studies on the original 45S5 Bioglass formulation determined that a permanent stable bond to bone could be established in animal models, which has led to Bioglass being marketed and applied in the medical field as glass particulates and pastes.^{11,12}

Bioactive glasses are characterized by the ability to promote healing within the body owing to the dissolution of the glass surface and ion exchange upon exposure to physiological medium or body fluids.^{13,14} The precise mechanism includes soluble Si being released into the surrounding medium in the form of silicic acid owing to

ion exchange with H⁺ and H₂O.¹⁰ This subsequently results in the precipitation of a carbonated hydroxyapatite layer (HCA) after prolonged exposure to biological fluids. This precipitated surface layer is regarded as being responsible for the strong bond between the bioactive glass and the host bone.^{14,15} It has also been established that the ionic dissolution products from 45S5 Bioglass and other silicate-based glasses can stimulate angiogenesis and the expression of several genes of osteoblast cells.¹⁵ Therefore, developing materials intended for bone regeneration that upregulate the expression of genes that promotes osteoblast biomineralization and osteocalcin expression are greatly desired.¹⁶ A recent publication on the genetic design of bioactive glasses by Hench hypothesizes that the ionic dissolution products released from bioactive glasses stimulate the genes of cells toward a path of regeneration and self-repair. Since the discovery of 45S5 Bioglass ability to bond to bone, a shift in thinking from interfacial bonding to bone regeneration has evolved.¹⁷

However, prior to investigating either of these mechanisms with novel bioactive glass compositions, a number of characteristics of the glass need to be characterized and

Correspondence to: A. W. Wren; e-mail: wren@alfred.edu

TABLE I. Composition of Glass Series (Mol. Fraction)

	Con.	TW-I	TW-II	TW-III	TW-IV
SiO ₂	0.50	0.45	0.40	0.35	0.30
TiO ₂	0.00	0.05	0.10	0.15	0.20
Na ₂ O	0.18	0.18	0.18	0.18	0.18
CaO	0.32	0.32	0.32	0.32	0.32

evaluated including glass structure, solubility and ion release, surface area, pH changes, and preliminary studies in established *in vitro* models. In relation to glass structure, it has previously been determined that the concentration of nonbridging oxygen (Si–O–NBO) species is directly related to the solubility of the glass.¹⁸ Specific cations can play a complex structural role in oxide glasses, allowing them to influence the physical and chemical properties of the resulting glass.^{19,20} Although the glass structure can significantly affect the dissolution, ion release, and pH, the exposed surface area of the glass particulates can also significantly affect the ion release.

The objective of this study is to characterize and determine any changes in the solubility of a series of titanium (Ti)-containing glasses as TiO₂ is substituted for SiO₂. Ti has been applied to numerous medical materials as it is known to promote apatite formation on the material surfaces when in contact with physiological fluids that is Ti-6Al-4V,^{21–23} Ti-gels,¹⁴ coatings,²⁴ and glasses.^{25–27} TiO₂ is incrementally added to the glass composition as there is a lack of understanding of the role of Ti within the human body. Ti metals are well characterized and are regarded as being more biologically acceptable that resist corrosion and ion-leaching which results in nonimmunogenicity. It has also been cited as being bioinert, and as having higher bone-healing qualities than other medical grade metals.²⁸ The Ti ion, however, is not present naturally in the human body, and as such its specific role is not well documented. There have been studies on the effect of Ti ion in cells such as monocytes/macrophages²⁹ and leukocytes resulted in no significant changes in cell viability.³⁰ Additional studies in monocyte-derived dendritic cells resulted in increased T-lymphocyte activity.³¹ Additionally, testing in cell lines more relevant to bone (osteoblast like ROS) resulted in increased expression of alkaline phosphatase, osteopontin, and osteonectin, and hence indicating their role as promoters of osteoblast differentiation.^{32,33} Ion concentration from these studies cite that the 0.1–10 ppm Ti levels did not significantly alter cell viability; however, decreases were evident when the concentration reached 20 ppm.³⁴

With respect to this study, a number of important characteristics pertaining to ion release will be investigated, that is *glass composition, particle size, exposed surface area, and incubation time*. It is generally accepted that by reducing the *particle size*, the surface area increases and there is an associated increase in particle surface dissolution. Also, this study examines whether the changes in the *exposed surface area* of the glass particles (with the same particle size range) result in significant changes in ion release. Both of

these effects will be investigated as a function of *incubation time* in aqueous media and also as a function of *glass composition*. The effects of these parameters will be investigated by monitoring any changes in pH, glass composition, and the subsequent effect on cytocompatibility.

MATERIALS AND METHODS

Glass synthesis

Five glass compositions were formulated for this study with the principal aim of investigating the substitution of SiO₂ with TiO₂ throughout the glass series. A CaO–Na₂O–SiO₂ glass was used as a control (*Con.*), whereas the experimental glasses denoted *TW-I*, *TW-II*, *TW-III*, and *TW-IV* contain incremental concentrations of TiO₂ at the expense of SiO₂. Glasses were prepared by weighing out appropriate amounts of analytical grade reagents and ball milling (1 h). The mix was then oven dried (100°C, 1 h) and fired (1500°C, 1 h) in a platinum crucible and shock quenched into water. The resulting frit was dried, ground, and sieved to retrieve glass powders with particle size of <45 μm and between ~90–710 μm, which is the particle size range of Bioglass (Table I).

Glass characterization

X-ray diffraction. Diffraction patterns were collected using a Philips Xpert MPD Pro 3040/60 X-ray Diffraction Unit (Philips, The Netherlands). Disk samples (32 mm Ø × 3 mm) were prepared by pressing a selected glass powder (<45 μm) into a backing of ethyl cellulose (8 ton, 30 s). Samples were then placed on spring-back stainless steel holders with a 10-mm mask and were analyzed using Cu Kα radiation. A generator voltage of 40 kV and a tube current of 35 mA were employed. Diffractograms were collected in the range 10° < 2θ < 70°, at a scan step size of 0.0083° and a step time of 10 s. Any crystalline phases present were identified using JCPDS (Joint Committee for Powder Diffraction Studies) standard diffraction patterns.

Differential thermal analysis. A combined differential thermal analyzer–thermal gravimetric analyzer (DTA-TGA) (Stanton Redcroft STA 1640, Rheometric Scientific, Epsom, United Kingdom) was used to measure the glass transition temperature (*T_g*) for each glass. A heating rate of 10°C/min was employed using an air atmosphere with alumina in a matched platinum crucible as a reference. Sample measurements were carried out every 6 s between 30 and 1300°C.

Surface area determination. To determine the surface area of the glasses, the advanced surface area and porosimetry, ASAP 2010 System analyzer (Micrometrics Instrument, Norcross, GA) was employed. Approximately, 60 mg of each set glass was used to calculate the specific surface areas, 1 m², using the Brunauer–Emmett–Teller method where *n* = 3 measurements were taken for each sample.

Particle size analysis. Particle size analysis was conducted on the <45 μm particles using a Beckman Coulter Multi-sizer 4 Particle size analyzer (Beckman Coulter, Fullerton,

CA). Glass powder samples were evaluated in the range of 0.4–100.0 μm with a run length of 60 s, with 30 k counts per measurement. The suspension fluid used was a NaCl solution at a temperature range between 10 and 37°C. The relevant volume statistics were calculated on each glass.

Sample preparation

Preparation of extracts. Liquid extracts were used for evaluating ion release profiles, changes in pH, and cell culture studies. This was achieved by immersing 1 and 3 m^2 of glass in 10-mL sterile deionized water for 1, 7, and 14 days. Approximately, 50 g of each glass (*Con.*, *TW-I*, *TW-II*, *TW-III*, and *TW-IV*) was sterilized using γ -irradiation at 25kGray (Isotron, Mayo, Ireland) prior to forming cell-culture extracts. Samples ($n = 3$) were aseptically immersed in appropriate concentrations of sterile deionized water and agitated at ($37 \pm 2^\circ\text{C}$) for 1, 7, and 14 days. For cytotoxicity testing, 100 μL of aliquots ($n = 3$) of extract were removed after each time period by centrifugation.

X-ray photoelectron spectroscopy sample preparation. Samples were prepared for X-ray photoelectron spectroscopy (XPS) analysis by immersing 1 m^2 surface area of each glass, *Con.*, *TW-I*, *TW-II*, *TW-III*, and *TW-IV* in 10 mL of sterile deionized water. Samples ($n = 3$) were agitated at ($37 \pm 2^\circ\text{C}$) for 1, 7, and 14 days after which water was removed by centrifugation and the glass powder dried for 24 h at $37 \pm 2^\circ\text{C}$ in an air-assisted oven. Dried powder samples were analyzed using XPS to determine any changes in composition with respect to maturation in an aqueous environment.

Atomic absorption spectroscopy

The sodium (Na), silica (Si), calcium (Ca), and titanium (Ti) concentration of the water extracts that contained the glass particles for 1, 7, and 14 days were measured using an Atomic Absorption Spectrometer (Varian SpectraAA-44-400). Standard solutions were used for calibration of the system. NaCl was added to Sr and Na solutions, whereas LaCl was added to Ca solutions to inhibit ionization of these elements. Three measurements were taken from each aliquot to determine the mean concentration of each element for each incubation period.

pH analysis. Changes in pH of solutions were monitored using a Corning 430 pH meter. Prior to testing, the pH meter was calibrated using pH buffer solution 4.00 ± 0.02 and 7.00 ± 0.02 (Fisher Scientific, Pittsburgh, PA). Sample solutions were prepared by exposing glass samples (1 and 3 m^2 surface area, $n = 3$) in 10 mL of sterile deionized water. Three samples were measured for each time period and were recorded at 0, 1, 7, and 14 days. Sterile deionized water was used as a control and was measured at each time period.

X-ray photoelectron spectroscopy

X-ray photoelectron spectroscopy was performed in a Kratos AXIS 165 spectrometer (Kratos Analytical, Manchester, United Kingdom) using monochromatic Al $K\alpha$ radiation ($h\nu = 1486.6$ eV). Glass powder was investigated after each incubation period (1, 7, and 14 days). Surface charging was

minimized by flooding the surface with low-energy electrons. The C 1s peak of adventitious carbon at 284.8 eV was used as a charge reference to calibrate the binding energies. High-resolution spectra were taken at pass energy of 20 eV, with step size of 0.05 eV, and 100 ms of dwell time.

In vitro assessment of glass extracts

The established cell line L-929 (American Type Culture collection CCL 1 fibroblast, NCTC clone 929) was used in this study as required by ISO10993 part 5. Cells were maintained on a regular feeding regime in a cell-culture incubator at $37^\circ\text{C}/5\%$ $\text{CO}_2/95\%$ air atmosphere. The culture media used was M199 media (Sigma Aldrich, Ireland) supplemented with 10% of fetal bovine serum (Sigma Aldrich, Ireland) and 1% (2 mM) L-glutamine (Sigma Aldrich, Ireland). The cytotoxicity of liquid extracts was evaluated using the methyl tetrazolium (MTT) assay in 24-well plates. In brief, 100 μL aliquots of undiluted extract from (particles: 1 m^2 45 μm , and 1 m^2 710 μm) were added into wells containing L929 cells in culture medium in triplicate. The prepared plates were incubated for 24 h at $37^\circ\text{C}/5\%$ CO_2 . The MTT assay was then added in an amount equal to 10% of the culture medium volume/well. The cultures were then reincubated for a further 2 h ($37^\circ\text{C}/5\%$ CO_2). Next, the cultures were removed from the incubator and the resultant formazan crystals were dissolved by adding an amount of MTT solubilization solution (10% Triton x-100 in acidic isopropanol [0.1 N HCl]) equal to the original culture medium volume. Once the crystals were fully dissolved, samples were transferred to 96-well plates and the absorbance was measured at a wavelength of 570 nm. In brief, 100 μL aliquots of sterile deionized water were used as controls, and cells were assumed to have metabolic activities of 100%.

Statistical analysis

Correlation coefficients were calculated using OriginPro 8SR2 2008 and were determined to investigate any relationship between Ti concentration within the glass (composition) and ion release (Si^{4+} , Ca^{2+} , and Na^+) at each time period that is 1, 7, and 14 days. One-way analysis of variance (ANOVA) was conducted using SPSS Statistical Software Ver. 17.0 2008 to determine any changes in ion release levels with respect to glass composition (*Control vs. TW-IV*), pH as a function of glass composition (*Control vs. TW-IV*), and maturation in aqueous media (*0-14 days*). Additionally, statistical comparisons were conducted to determine if significant changes in cell viability were evident between a growing control cell population and each glass composition at 1, 7, and 14 days. Comparison of relevant means was performed using the Bonferroni *post hoc* test. Differences between groups were deemed significant when $p \leq 0.05$.

RESULTS

Structure of Ti-glass series

Each glass was initially characterized using X-ray diffraction (XRD) and differential thermal analysis (DTA). XRD data are shown in Figure 1 and are conducted on glass samples before and after γ -sterilization to determine any changes or evolution of crystal phases. As shown in Figure 1(a), it is evident that each glass is fully amorphous with the exception of *TW-IV*,

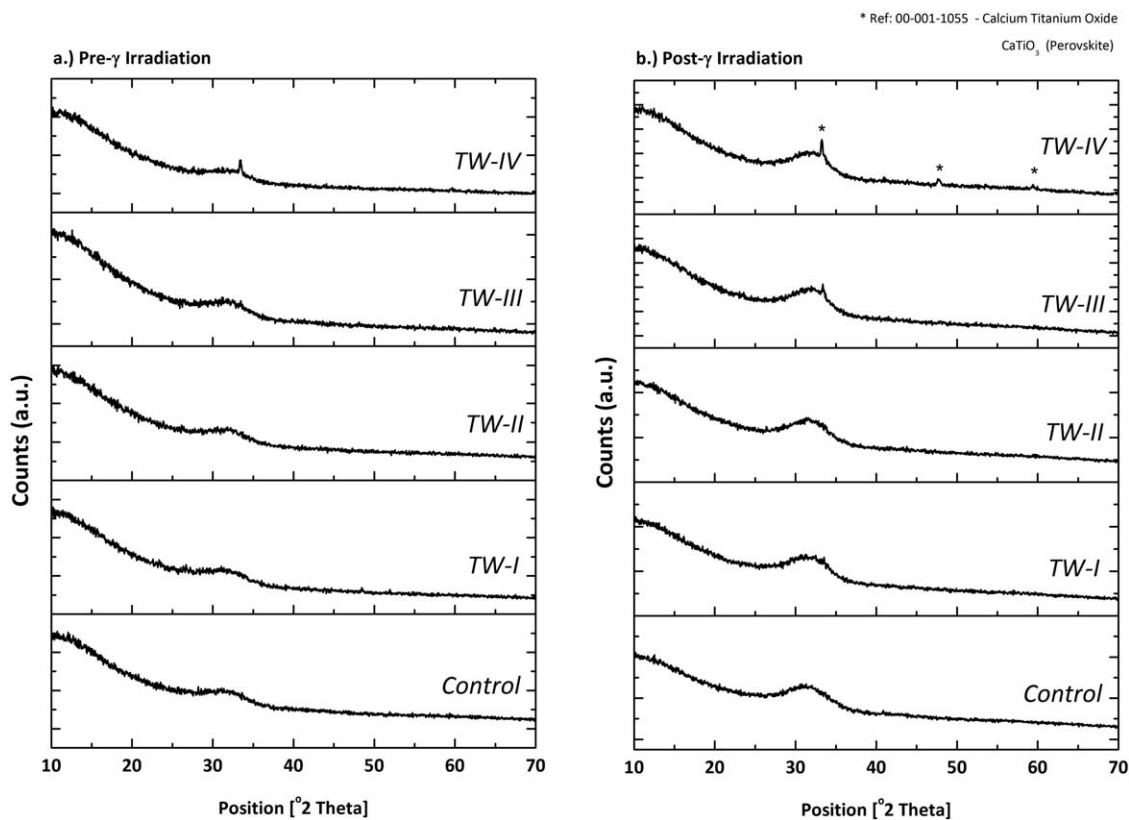


FIGURE 1. XRD traces of (a) pre- γ -irradiated glass and (b) post- γ -irradiated glass.

which has a single diffraction peak at $33^\circ 2\theta$. Poststerilization [Fig. 1(b)], each glass was amorphous with the exception of TW-IV, which had diffraction peaks at $33^\circ 2\theta$, $47^\circ 2\theta$, and $59^\circ 2\theta$ which were identified as CaTiO₃. DTA was also conducted on each of the glasses and the thermal profiles are shown and summarized in Figure 2 and Table II. As summarized in Table II, it is evident that the addition of TiO₂ results in a decrease in the glass transition temperature (T_g). The T_g was found to reduce from 594°C (Con) to 570°C (TW-IV) as the TiO₂ concentration is increased from 0 to 20 mol %. A similar trend was observed with the crystallization temperature (T_c) where a decrease in T_c was evident from 712 to 655°C (Con – TW-IV) with the addition of TiO₂. The melting temperature (T_m) did not present a clear trend and ranged from 1146 to 1198°C . Specific surface area was determined for both particle size ranges where $45\ \mu\text{m} = 0.85 \pm 0.012\ \text{m}^2/\text{g}$ and $710\ \mu\text{m} = 0.13 \pm 0.002\ \text{m}^2/\text{g}$. Particle size analysis was performed on each of the $<45\ \mu\text{m}$ glass compositions (Table III) where the mean glass particle sizes were $2.9\ \mu\text{m}$ (Con), $4.1\ \mu\text{m}$ (TW-I), $4.0\ \mu\text{m}$ (TW-II), $3.4\ \mu\text{m}$ (TW-III), and $3.7\ \mu\text{m}$ (TW-IV). Statistical comparisons between each glass composition did not determine any significant difference in particle size ($p = 0.192\text{--}1.000$).

Effect of particle size and exposed surface area on ion release

Investigating 710 μm ion release profiles. Ion release data are presented with respect to (1) *exposed surface area*, (2)

maturation, (3) *glass composition*, and (4) *particle size*. Figure 3 shows the ion release profiles of the $710\text{-}\mu\text{m}$ particles for each glass after 1, 7, and 14 days, respectively. Calcium (Ca²⁺) release is shown in Figure 3(a) ($1\ \text{m}^2$) and Figure 3(b) ($3\ \text{m}^2$). Figure 3(a) shows $1\ \text{m}^2$ exposed surface area where Ca²⁺ release ranged from 0 to 4 mg/L (1 day), 3–12 mg/L (7 days), to 6–29 mg/L for 14 days. Figure 3(b) shows $3\ \text{m}^2$ surface area data, where Ca²⁺ release ranged from 2–9 mg/L (1 day), 4–21 mg/L (7 days), to 6–30 mg/L

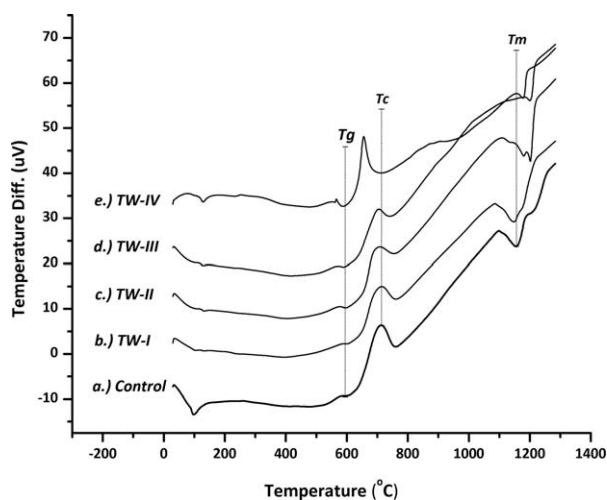


FIGURE 2. Thermal profiles of Ti-glass series.

TABLE II. Thermal Characteristics (°C) of Glass Series Including T_g , T_c , and T_m

	T_g	T_c	T_m
Con.	594	712	1154
TW-I	594	711	1146
TW-II	586	704	1197
TW-III	580	708	1198
TW-IV	570	655	1175

for 14 days. Ca^{2+} release was found to reduce with increasing TiO_2 concentration (*Con* – *TW-IV*) in the glass. Sodium (Na^+) release is shown in Figure 3(c) for the 1 m^2 surface area where release rates ranged from 11–17 mg/L (1 day), 21–33 mg/L (7 days), to 16–38 mg/L for 14 days, Figure 3(d) shows Na^+ release with greater exposed surface area (3 m^2). Na^+ release ranged from 18–34 mg/L (1 day), 24–46 mg/L (7 days), to 32–43 mg/L for 14 days. Na^+ did not present any specific trend with respect to glass composition. Si^{4+} release profiles are shown in Figure 3(e,f). Figure 3(e) shows the $710 \mu\text{m}$ 1 m^2 data which show Si^{4+} release which ranged from 7–25 mg/L (1 day), 18–49 mg/L (7 days), to 12–32 mg/L after 14 days. Figure 3(f) shows the 3 m^2 surface area data which ranged from 11–20 mg/L (1 day), 20–60 mg/L (7 days), to 20–41 mg/L for 14 days. Si^{4+} release did not present predictable release profiles when compared to Ca^{2+} .

Investigating $45 \mu\text{m}$ ion release profiles

Ion release profiles for the $45\text{-}\mu\text{m}$ particle size for each glass are shown in Figure 4. Figure 4(a) presents the $45\text{-}\mu\text{m}$ 1 m^2 particles where Ca^{2+} release ranged from 1–45 mg/L (1 day), 3–60 mg/L (7 days), to 7–64 mg/L for 14 days. Figure 4(b) shows the 3 m^2 particles where Ca^{2+} release ranged from 3–38 mg/L (1 day), 4–49 mg/L (7 days), to 4–69 mg/L for 14 days. With respect to Ca^{2+} release, the *Con* was the most soluble and *TW-IV* was the least soluble. Na^+ release is shown in Figure 4(c) for the 1 m^2 , $45 \mu\text{m}$ particle size which ranged from 43–58 mg/L (1 day), 61–79 mg/L (7 days), to 65–76 mg/L after 14 days. Figure 4(d) shows the Na^+ release from 3 m^2 surface area where release levels ranged from 102–128 mg/L (1 day), 131–149 mg/L (7 days), to 143–159 mg/L for 14 days. With respect to Na^+ release, the increase in surface area presented an increase in ion release rate. Si^{4+} release is shown in Figure 4(e) for 1 m^2 surface area which ranged from 23–56 mg/L (1 day), 22–76 mg/L (7 days), to 25–58 mg/L after 14 days. Figure 4(f) shows 3 m^2 surface area where Si^{4+} levels ranged from 33–60 mg/L (1 day), 33–83 mg/L (7 days), to 33–71 mg/L

TABLE III. Mean Particle Size and S.D. of $<45 \mu\text{m}$ Glass Particles

	Mean (μm)	S.D.
Con.	2.97	1.06
TW-I	4.11	1.26
TW-II	4.02	1.34
TW-III	3.40	0.99
TW-IV	3.74	1.16

for 14 days. No observable trend was evident based on the difference in glass composition.

Effect of ion release on pH, glass composition, and cell viability

Any change in pH was recorded and is summarized in Tables IV and V, in addition to relevant statistical comparisons. Table IV summarizes the pH values for the $710 \mu\text{m}$ 1 m^2 , which shows that the pH ranged between 9.9 and 11.0, whereas Table V summarizes the pH values for the $710 \mu\text{m}$ 3 m^2 , which ranged from 10.2 to 11.1. A similar trend is observed with the $45 \mu\text{m}$ 1 m^2 particles (Table VI), which shows a slightly higher pH range of 10.4–11.5. Table VII summarizes the $45 \mu\text{m}$ 3 m^2 particles, which shows a similar pH distribution of 10.4–11.7. There were no observable trends with respect to pH, as the pH changes showed little difference in all samples between 0 and 14 days for each glass composition. To investigate any changes in composition as a function of incubation time, XPS was performed on the dried glass powders (Fig. 5). Figure 5 shows compositional data of *Con*, *TW-II*, and *TW-IV* after 0, 1, 7, and 14 days of incubation in sterile deionized water. As shown in Figure 5(a) after 1 day, the Si^{4+} concentration was found to decrease, whereas the Na^+ concentration increases. However, after 7 days, the Si^{4+} levels increase, whereas the Na^+ levels reduce, which then remains constant until 14 days. This trend is also shown in Figure 5(b,c). Cytotoxicity testing was conducted using L929 fibroblasts on the 1 m^2 $710 \mu\text{m}$ and $45 \mu\text{m}$ glass particles in that were immersed in liquid extracts for 1, 7, and 14 days. Figure 6(a,b) shows cell-culture results which suggest that (1) glasses with increased Ti^{4+} concentration present higher cell viability, and (2) the $45 \mu\text{m}$ particles presented overall higher cell viability than the $710 \mu\text{m}$ particles. The highest cell viability was determined for *TW-IV* (+29%) at 1 day for the $710 \mu\text{m}$, and also the $45 \mu\text{m}$ *TW-IV* at 14 days which presented cell viability of 44% higher than the growing cell population.

DISCUSSION

Structure of Ti-glass series

This glass series was synthesized to investigate how *surface area*, *particle size*, and *incubation time* affect the solubility of $\text{SiO}_2\text{-CaO-Na}_2\text{O}$ glasses as SiO_2 is substituted with TiO_2 . Studies on the solubility of Bioglass have been previously published; however, this study investigates specifically how the addition of TiO_2 affects the ion release/solubility and related bioactivity. Prior to determining the solubility of each of the glasses, a preliminary study into the glass structure was conducted to determine any changes as a function of TiO_2 incorporation. XRD presented predominantly amorphous materials (Fig. 1); however, a low degree of crystallinity was evident in the higher TiO_2 -containing glasses where the addition of the crystal phases is likely owing to γ -irradiation exposure. DTA (Fig. 2 and Table II) presented the differences in thermal characteristics with an increase in TiO_2 concentration. The reduction of the T_g and T_c with the increase in TiO_2 concentration may be attributed to the depolymerization of Si-O-Si bonds within the glass network, which suggests that TiO_2 is acting predominantly as a

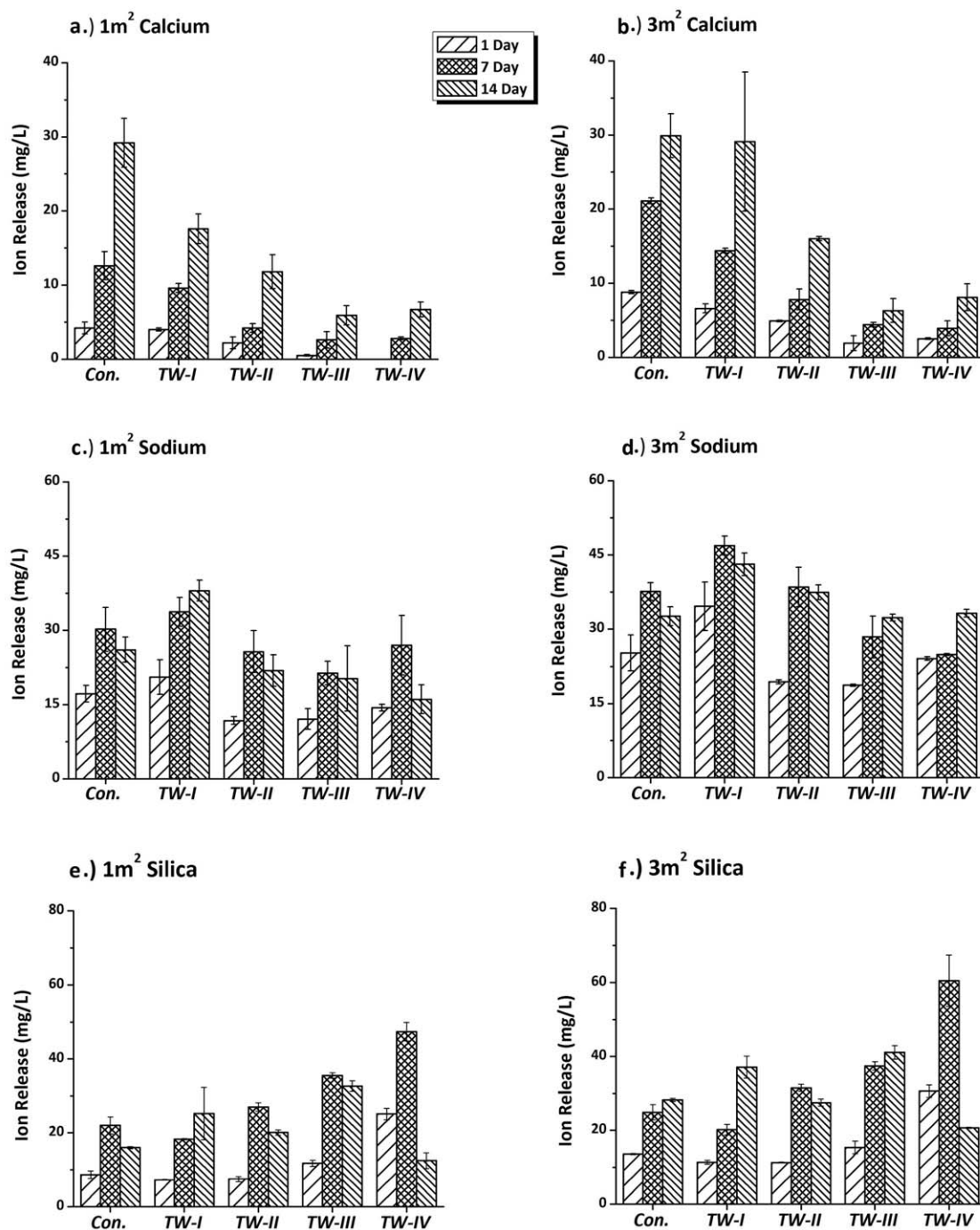


FIGURE 3. Ion release profiles of 710 μm glass extracts exposed to (a) 1 m² and (b) 3 m² surface area.

network modifier. The previous studies on CaO–SrO–ZnO–SiO₂/TiO₂ glasses by the authors support these findings by utilizing XPS and Raman spectroscopy in addition to thermal analysis.²⁰

Effect of particle size and exposed surface area on ion release

Investigating 710 μm ion release profiles. Calcium (Ca²⁺) release is an important ion to consider as it is known to

promote dissolution of the glass particles in addition to being essential for encouraging precipitation of bioactive calcium phosphate surface layer.^{14,18} Additionally, Ca²⁺ is cited to favor osteoblast proliferation, differentiation, and extracellular mineralization in addition to activating Ca-sensing receptors in osteoblast cells increasing the expression of growth factors.¹⁵ It is initially evident that the Ca²⁺ release [Fig. 3(a)] is highly dependent on the composition of the glass. As the TiO₂ concentration increases, the Ca²⁺

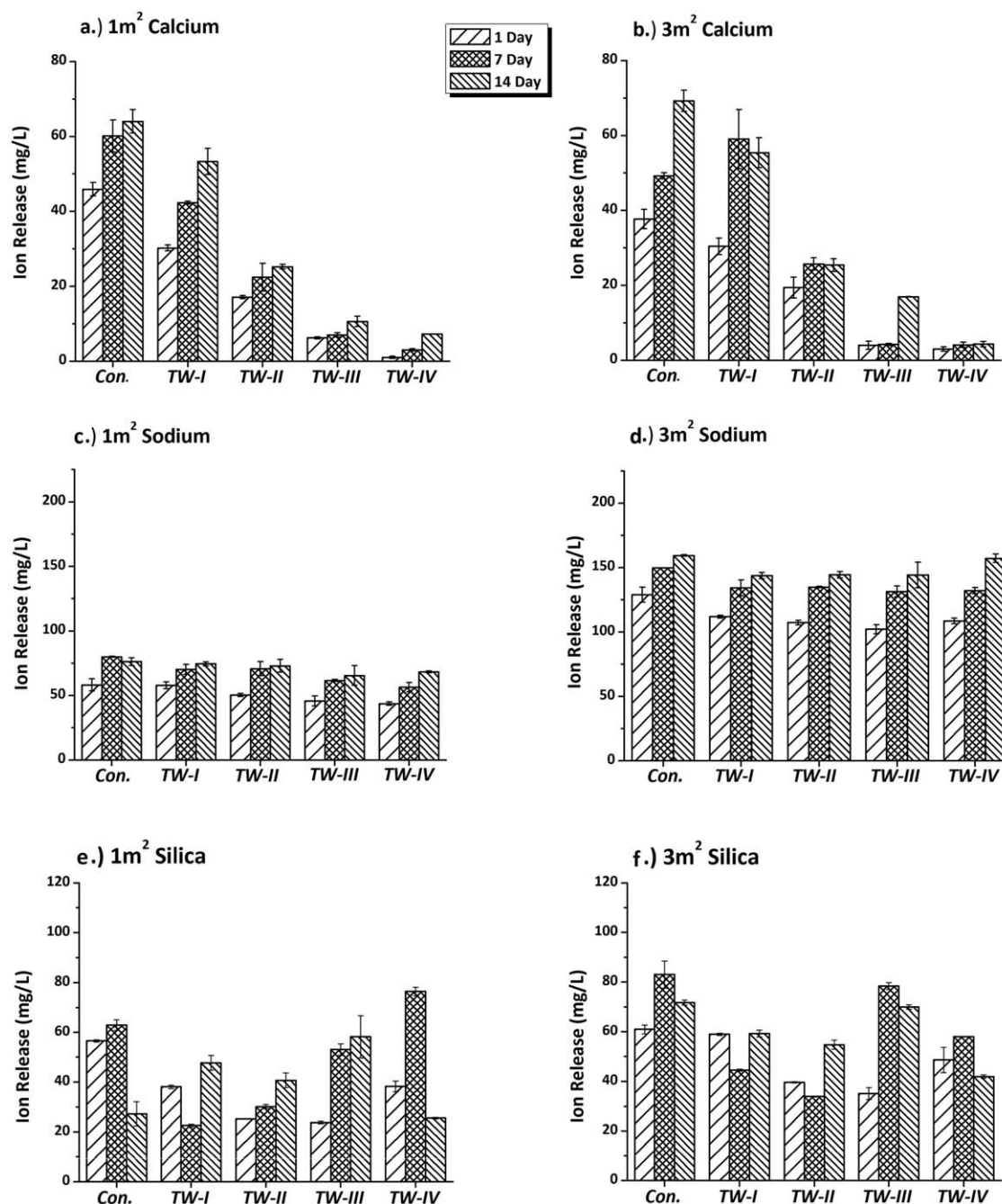


FIGURE 4. Ion release profiles of 45 μm glass extracts exposed to (a) 1 m^2 and (b) 3 m^2 surface area.

release rate decreases. For 1-day samples, the Ca^{2+} release rates presented a correlation coefficient ($R^2 = 0.95$), suggesting that the release rate is highly dependent on the composition, where 7 and 14 days presented R^2 -values of 0.80 and 0.83, respectively. The 3 m^2 [Fig. 3(b)] surface area shows a similar trend to the 1 m^2 data set [Fig. 3(a)]; however, the Ca^{2+} release is higher, which is likely owing to the increase in exposed surface area. Similar to the 1 m^2 , the *Con* glass displayed the highest Ca^{2+} release rate at each time period and correlation coefficients were $R^2 =$

0.84 (1 day), 0.87 (7 days), and 0.83 (14 days). When statistically comparing the *Con* (Ti free) glass to *TW-IV* (highest Ti-containing glass), there was found to be a significant reduction in Ca^{2+} release for both the 1 m^2 at each time period, 1 day ($p = 0.027$), 7 days ($p = 0.012$), and 14 days ($p = 0.034$), and the 3 m^2 surface area, also at each time period, 1 day ($p = 0.000$), 7 days ($p = 0.000$), and 14 days ($p = 0.005$). From the 1 m^2 Na^+ release profiles [Fig. 3(c)], it is evident that there is an increase in Na^+ release after 1 day; however, little difference exists between 7 and 14 days,

TABLE IV. pH Values of 710 μm 1 m^2

	Con.	TW-I	TW-II	TW-III	TW-IV	Con versus TW-IV
0	10.4 (0.12)	10.4 (0.09)	10.0 (0.24)	10.0 (0.16)	9.97 (0.02)	0.041*
1 Day	10.6 (0.06)	11.0 (0.06)	10.8 (0.19)	10.1 (0.04)	10.3 (0.05)	0.057
7 Day	10.7 (0.09)	11.0 (0.12)	10.8 (0.09)	10.3 (0.06)	10.3 (0.03)	0.002*
14 Days	10.5 (0.24)	11.0 (0.08)	10.7 (0.13)	10.5 (0.05)	10.4 (0.15)	1.000
0 Versus 14 days	1.000	0.000*	0.009*	0.001*	0.001*	

suggesting that the majority of Na^+ release is experienced after 1 day. As shown in Figure 3(d), it is clear that the increase in exposed surface area results in minor changes in the Na^+ release. Means comparison testing between *Con* and *TW-IV* was determined to be significant only at 7 days, with 3 m^2 surface area ($p = 0.047$). Silica (Si^{4+}) release is also considered as it is known to have a number of positive effects when introduced into the human body.¹⁵ Si^{4+} is known to be essential for the formation and calcification of bone tissue and is known to increase bone mineral density. Aqueous Si^{4+} is also known to induce HAp precipitation and $\text{Si}(\text{OH})_4$ stimulates collagen I formation and osteoblastic differentiation.¹⁵ Si^{4+} release profiles did not present any predictable trends with either the 1 or the 3 m^2 [Figure 3(e,f)]. There were minor differences evident with Si^{4+} release with respect to increases in exposed surface area; however, no observable trend was evident. Si^{4+} release from Bioglass (with similar particle size, $\sim 710 \mu\text{m}$) determined levels at 5 mg/L after 1 day, 20 mg/L at 7 days, and 45 mg/L after 30 days,³⁵ which presents a similar ion release distribution with regard to this study; however, the effect of 30-day incubation has not yet been conducted for our samples which makes direct comparison difficult. Studies by Talo et al.³⁶ determined that Ca^{2+} and PO_4^{3-} ion release was greatly affected by the addition of TiO_2 (particularly, $>10 \text{ mol } \%$), Si^{4+} release was found to be a continuous process and less dependent on TiO_2 concentration, which supports the findings within this study.

Investigating 45 μm ion release profiles

Ca^{2+} release [Fig. 4(a)] presents a similar trend to the Ca^{2+} release profiles shown in Figure 3 in which a decrease in Ca^{2+} release is evident as the TiO_2 concentration in the glass increased. The R^2 -values presented a strong correlation coefficient of $R^2 = 0.96$ (1 day), 0.94 (7 days), and 0.91 (14 days), suggesting a strong dependency on glass composition. Also, the 3 m^2 [Fig. 4(b)] Ca^{2+} release presented a similar trend to the 1 m^2 data [Fig. 4(a)], R^2 -values of 0.94, (1 day), 0.76 (7 days), and 0.94 (14 days); however, minor difference

in Ca^{2+} levels was observed, even as the exposed surface area was increased threefold. When statistically comparing the *Con* glass to *TW-IV*, a significant reduction in Ca^{2+} release for both the 1 m^2 at each time period, 1 day ($p = 0.000$), 7 days ($p = 0.001$), and 14 days ($p = 0.000$), and for the 3 m^2 , also at each time period, 1 day ($p = 0.002$), 7 day ($p = 0.000$), and 14 days ($p = 0.000$) was observed. With respect to the previous studies on Bioglass, Ca^{2+} levels ranged from 7.5 mg/L (1 day), 10 mg/L (7 days), to 16 mg/L (30 days),³⁵ which are comparable to the Ca^{2+} release rates from these glasses. A recent review by Hoppe et al.¹⁵ cites that low (3–7 mg/L) and medium (10–14 mg/L) Ca^{2+} concentrations are suitable for osteoblast proliferation, differentiation, and extracellular matrix formation, whereas higher Ca^{2+} concentrations (18 mg/L) are cytotoxic. Also, a previous study by Talo et al.³⁶ on sol-gel-derived xerogels investigated Ti^{4+} effect on ion release. This study determined that the incorporation of TiO_2 resulted in improving sol-gel stability and that the release of Ca^{2+} and PO_4^{3-} ions was highly dependent on TiO_2 concentration. Stability was achieved as hydration susceptible P–O–P bonds were partially replaced by hydration-resistant P–O–Ti. As Ti^{4+} ions have a small ionic radius and a large electric charge, they can be easily integrated into the glassy network and form stronger P–O–Ti bonds compared to P–O–P bonds.³⁶ It may also be possible that the large electric charge of the Ti^{4+} ion is charge compensated preferentially by Ca^{2+} , which would explain the reduction in Ca^{2+} release as the TiO_2 concentration increases. It can be determined from the Ca^{2+} release data, and statistical comparisons, that the inclusion of Ti^{4+} greatly reduces Ca^{2+} solubility from these glasses.

Na^+ release [Fig. 4(c)] from the 1 m^2 45 μm particle size resulted in a much higher release rate than the 1 m^2 710 μm particle size. The highest Na^+ release rate attributed to the 3 m^2 [Fig. 4(d)] was attributed to the *Con* after 14 days (159 mg/L). Regarding Na^+ release, mean comparison between *Con* and *TW-IV* reached significance only for 1 m^2 , 1 day ($p = 0.048$), 3 m^2 1 day ($p = 0.036$), and 3 m^2

TABLE V. pH Values of 710 μm 3 m^2

	Con.	TW-I	TW-II	TW-III	TW-IV	Con versus TW-IV
0	10.6 (0.15)	10.6 (0.02)	10.4 (0.15)	10.4 (0.07)	10.4 (0.06)	0.267
1 Day	10.9 (0.02)	11.1 (0.04)	10.9 (0.11)	10.5 (0.07)	10.7 (0.10)	0.064
7 Day	10.9 (0.14)	11.0 (0.15)	11.0 (0.11)	10.4 (0.13)	10.2 (0.33)	0.025 ^a
14 Days	10.8 (0.10)	11.1 (0.09)	11.0 (0.09)	10.8 (0.05)	10.4 (0.19)	0.021 ^a
0 Versus 14 days	0.142	0.001 ^a	0.006 ^a	0.003 ^a	1.000	

^asignificant at $p \leq 0.05$.

TABLE VI. pH Values of 45 μm 1 m^2

	Con.	TW-I	TW-II	TW-III	TW-IV	Con versus TW-IV
0	10.9 (0.13)	10.9 (0.01)	10.9 (0.14)	10.7 (0.05)	10.7 (0.15)	0.683
1 Day	10.9 (0.02)	11.5 (0.13)	11.1 (0.06)	10.7 (0.09)	10.6 (0.13)	0.031*
7 Days	10.6 (0.09)	11.5 (0.04)	11.0 (0.06)	10.7 (0.09)	10.4 (0.11)	0.067
14 Days	10.6 (0.16)	11.1 (0.10)	11.0 (0.08)	10.7 (0.06)	10.5 (0.08)	1.000
0 Versus 14 days	0.064	0.053	1.000	1.000	0.487	

7 day ($p = 0.003$). The Na^+ release profiles demonstrated here are slightly lower than Bioglass which ranges from 190 to 270 mg/L after 30 days³⁵; however, if tested at 30 days, the Na^+ release from these glasses may reach similar levels. Na^+ is known to be an important ion in the dissolution of bioactive glasses as it promotes depolymerization of Si—O—Si bonds within the glass network, which in turn promotes the ion exchange process.¹⁸ It is also possible that the Na^+ release is slowing down if it is approaching its solubility limit. Si^{4+} release [Fig. 4(e,f)] profiles demonstrate that an increase in exposed surface area results in little change in Si^{4+} release. Additionally, with respect to Si^{4+} release, there were no clear predictable trends observed with respect to changes in glass composition. Irrespective of each of the above parameters (*particle size, surface area, composition, and incubation time*) no Ti^{4+} was released from any of the glasses, or the release rate was below the detection limit of the instrument. The previous studies on phosphate-based glass incorporating TiO_2 found that by increasing the TiO_2 concentration, it resulted in an increase in T_g ²⁸ which is in contrast to the findings presented here, but may support finding by Talo et al. which suggests that the P—O—Ti bonds are more resistant to hydration breakdown.³⁶ Also, there was an associated reduction in the degradation rate and ion release of the glasses which was attributed to an increase in density. This resulted in a reduction in all ions released from the glass.²⁸ With respect to this study, however, only Ca^{2+} ion release is directly affected. Abu Neel et al. also investigated Ti^{4+} ion release from P_2O_5 — CaO — Na_2O glasses which contained up to 15 mol % of TiO_2 substituted for Na_2O and determined low-release rates ranging from 0.0060 to 0.0015 ppm.³⁷ It has been observed, however, that by substituting CaO with ZnO/SrO , Ti^{4+} ion release increases, where 1 mol % of SrO increases Ti^{4+} release from 0.0053 to 0.0617 ppm.³⁸

Effect of ion release on pH, glass composition, and cell viability. The effect of ion release can be documented by measuring the pH of the incubation media, by examining any changes in glass composition and evaluating the subsequent

effect on cell viability. The measurements of pH for the 710 μm 1 m^2 (Table IV) presents minor changes with respect to glass composition (Ti concentration) and maturation (0–14 days). Significant changes were evident with respect to composition, regarding Con versus TW-IV at 0 day ($p = 0.041$), and 7 days ($p = 0.002$). Significant differences were also evident with the Ti-containing glasses with respect to maturation at 0 versus 14 day, ($p = 0.000$ – 0.009). Similarly, the increase in exposed surface area (3 m^2 , Table V) was found to have little effect on the pH. These pH effects are likely owing to TiO_2 restricting the Ca^{2+} release from the glass, as Na^{2+} and Si^{4+} release profiles are consistent, where, as the Ca^{2+} release levels begin to reduce (Con vs. TW-IV), there is an associated reduction in pH, which is significant at longer incubation time periods, 7 days ($p = 0.025$) and 14 days ($p = 0.025$). The 45 μm particles 1 m^2 (Table VI) also presented insignificant changes with respect to composition (Con vs. TW-IV), with the exception of the 1-day samples ($p = 0.031$). There was no significant difference with respect to time (0–14 days) for all glasses. Additionally, the 3 m^2 (Table VII) surface area did not demonstrate a significant change in pH with respect to glass composition (Con vs. TW-IV), with the exception of 14-day samples ($p = 0.000$). There were minor significant changes determined with respect to maturation (0 vs. 14 days) for the Con ($p = 0.000$), TW-I ($p = 0.000$), and TW-II ($p = 0.001$). No significant differences were determined for TW-III ($p = 0.510$) and TW-IV ($p = 1.000$).

Analysis of the glass composition (Fig. 5) showed a reduction in Si^{4+} release and increase in Na^+ release at 1 day, which may be owing to soluble Si^{4+} being released from the glass particle surfaces, which could result in an increase in the detection of Na^+ levels. It was also observed that Si^{4+} levels increase at 7 days, whereas Na^+ levels were found to decrease. The precise mechanism is difficult to corroborate with ion release data as Na^+ levels remain constant, whereas Si^{4+} do not present any specific trend. Ca^{2+} levels were found to remain constant in the Con composition with no titanium (Ti^{4+}). With TW-II and TW-IV it is evident that with the addition of Ti^{4+} the Ca^{2+} levels increase in the glass for more than 7 and 14 days in particular,

TABLE VII. pH Values of 45 μm 3 m^2

	Con.	TW-I	TW-II	TW-III	TW-IV	Con versus TW-IV
0	11.0 (0.05)	11.1 (0.13)	11.0 (0.03)	10.9 (0.05)	10.9 (0.21)	0.905
1 Day	10.9 (0.10)	11.7 (0.08)	11.4 (0.07)	11.1 (0.07)	10.9 (0.05)	1.000
7 Day	10.9 (0.03)	11.6 (0.04)	11.0 (0.05)	11.0 (0.17)	10.7 (0.17)	0.398
14 Days	10.4 (0.05)	11.4 (0.06)	11.2 (0.03)	11.1 (0.06)	10.8 (0.04)	0.000 ^a
0 Versus 14 days	0.000 ^a	0.000 ^a	0.001 ^a	0.510	1.000	

^aSignificant at $p \leq 0.05$.

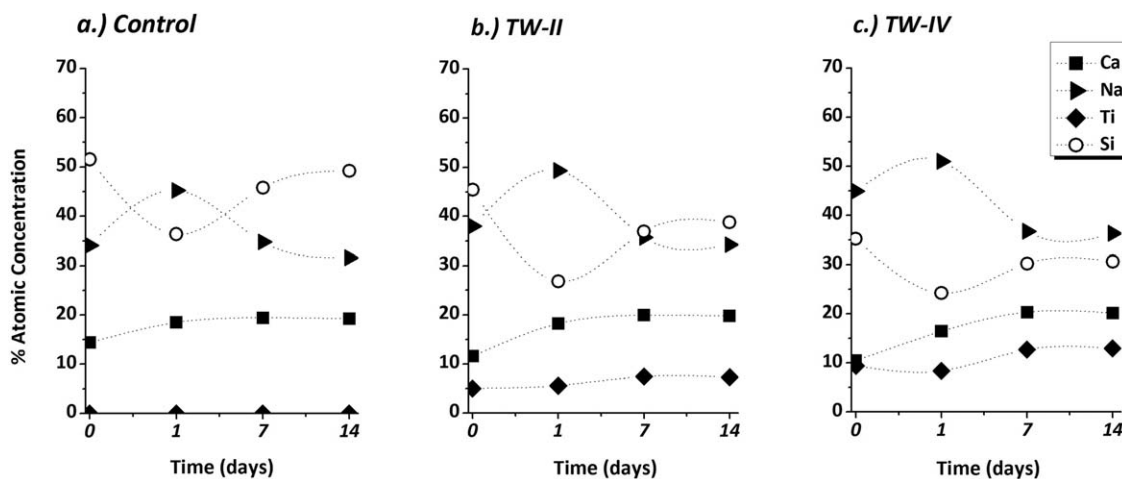


FIGURE 5. XPS composition of (a) Con. glass, (b) TW-II, and (c) TW-IV.

which corroborate ion release data where Ca^{2+} release is restricted by the addition of Ti^{4+} .

Cell viability analysis conducted on 710 μm glass [Fig. 6(a)] determined that when comparing the growing cell population to each glass, no significant difference was determined for the *Con* glass ($p = 0.222-1.000$) or *TW-II* ($p = 0.497-1.000$) at any time period. The highest Ti-containing glass, *TW-IV*, presented a significant increase in cell viability, 29% above the growing control cell population, after 1 day ($p = 0.016$), but no significant difference was observed at 7 days ($p = 1.000$) or 14 days ($p = 1.000$). Figure 6(b) shows the 45 μm particles' cell-culture results which show that cell viability is observed to increase with an increase in Ti^{4+} concentration. When comparing the control cell population to each glass composition at each time period, no significant difference was determined for the *Con* glass ($p = 0.501-1.000$) or *TW-II* ($p = 0.144-1.000$) at any time period. *TW-IV* also presented

no significant difference at 1 day ($p = 0.109$) and 7 days ($p = 1.000$); however, *TW-IV* at 14 days presented a significant ($p = 0.006$) increase in cell viability, 44% above the growing control cell population. Similar studies on Bioglass particles of the same size distribution presented cell viability of $\sim 80\%$ after 1, 7, and 30 days.³⁵ This finding supports earlier claims by Hoppe et al.¹⁵ that excessive Ca^{2+} release may be toxic to growing cells. This is evident within this study as the incorporation of TiO_2 in these glasses reduces Ca^{2+} release while simultaneously promoting cell growth. One observation that has been noted in the previous studies is that with an increase in TiO_2 concentration in phosphate glasses, the proliferation and adhesion of cells, particularly bone cells, on the glass surface improve considerably and that a decrease in ion release rate, associated with Ti incorporation, improved biocompatibility in terms of proliferation/adhesion of MG63 cells on glass surfaces.²⁸

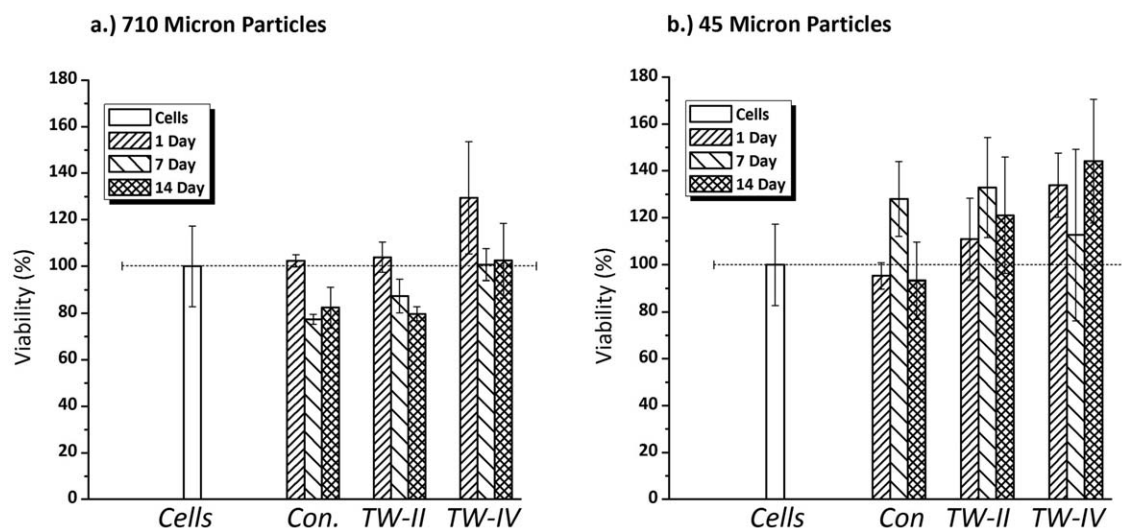


FIGURE 6. Cell-culture results of 1 m^2 , (a) 710 μm glass, and (b) 45 μm glass particles.

CONCLUSIONS

This study was conducted to characterize a series of Ti-containing bioactive glasses and to determine their solubility profiles and cellular response. Thermal profiles of each glass suggest that the addition of TiO₂ promotes NBO formation in the glass which should promote ion exchange and particle dissolution. Ion release profiles determined that ion release is not significantly increased with an increase in exposed surface area (with the exception of Na⁺ at 45 μm). Particle size significantly affects ion release where a reduction in particle size increases the dissolution rate. Na⁺ release presents little change after 7 and 14 days, suggesting that a solubility limit may be approached. Si⁴⁺ presents unpredictable release rates that are not dependent on glass composition or maturation. Ca²⁺ release is highly dependent on TiO₂ concentration in the glass and also increases with respect to maturation. Cell-culture results determine that cell numbers were higher in the TiO₂-containing glasses, which suggests that the addition of TiO₂ to bioactive glasses may be beneficial in controlling the ion release rate which can minimize the effect of excessive Ca²⁺ levels. Future studies will include determining the effect of the differing solubility on the formation on apatite, using simulated body fluid trials. In addition, osteoblast (MC3T3) differentiation will also be evaluated; however, for this follow-up study, polished glass plates will be used to permit the use of surface profiling techniques and to facilitate comparison between apatite growth and cell adhesion.

REFERENCES

- Chen QZ, Thompson ID, Boccaccini AR. 45S5 Bioglass[®]-derived glass-ceramic scaffolds for bone tissue engineering. *Biomaterials* 2006;27:2414–2425.
- Vargas GE, Mesones RV, Bretcanu O, López JMP, Boccaccini AR, Gorustovich A. Biocompatibility and bone mineralization potential of 45S5 Bioglass[®]-derived glass-ceramic scaffolds in chick embryos. *Acta Biomater* 2009;5:374–380.
- Haimi S, Gorianc G, Moimas L, Lindroos B, Huhtala H, Raty S, Kuokkanen H, Sandor GK, Schmid C, Miettinen, Suuronen R. Characterization of zinc-releasing three-dimensional bioactive glass scaffolds and their effect on human adipose stem cell proliferation and osteogenic differentiation. *Acta Biomater* 2009;5:3122–3131.
- Wren AW, Cummins NM, Laffir FR, Hudson SP, Towler MR. The bioactivity and ion release of titanium-containing glass polyalkenoate cements for medical applications. *J Mater Sci Mater Med* 2011;22:19–28.
- Wren AW, Cummins NM, Towler MR. Comparison of antibacterial properties of commercial bone cements and fillers with a zinc-based glass polyalkenoate cement. *J Mater Sci* 2010;45:5244–5251.
- Wren AW, Boyd D, Towler MR. The processing, mechanical properties and bioactivity of strontium based glass polyalkenoate cements. *J Mater Sci Mater Med* 2005;19:1737–1743.
- Anderson JH, Goldberg JA, Bessent RG, Kerr DJ, McKillop JH, Stewart I, Cooke TG, McArdle CS. Glass yttrium-90 microspheres for patients with colorectal liver metastases. *Radiother Oncol* 1992;25:137–139.
- da Costa Guimaraes C, Morales Mc, Roberto Martinelli J. Monte Carlo simulation of liver cancer treatment with 166Ho-loaded glass microspheres. *Rad Phys Chem* 2014;95:185–187.
- Bortot MB, Prastalo S, Prado M. Production and characterization of glass microspheres for hepatic cancer treatment. *Proc Mater Sci* 2012;1:351–358.
- Silver IA, Deas J, Erecinska M. Interactions of bioactive glasses with osteoblasts in vitro: Effects of 45S5 Bioglasses, and 58S and 77S bioactive glasses on metabolism, intracellular ion concentrations and cell viability. *Biomaterials* 2001;22:175–185.
- Hench LL. The story of bioglass. *J Mater Sci Mater Med* 2006;17:967–978.
- Jones JR. Review of bioactive glass: From Hench to hybrids. *Acta Biomater* 2013;9:4457–4486.
- Kokubo T, Kim H-M, Kawashita M. Novel bioactive materials with different mechanical properties. *Biomaterials* 2003;24:2161–2175.
- Kokubo T, Takadama H. How useful is SBF in predicting in vivo bone bioactivity. *Biomaterials* 2006;27:2907–2915.
- Hoppe A, Guldal NS, Boccaccini AR. A review of the biological response to ionic dissolution products from bioactive glasses and glass-ceramics. *Biomaterials* 2011;32:2757–2774.
- Saffarian Tousi N, Velten MF, Bishop TJ, Leong KK, Barkhordar NS, Marshall GW, Loomer PM, Aswath PB, Varanasi VG. Combinatorial effect of Si⁴⁺, Ca²⁺ and Mg²⁺ released from bioactive glasses on osteoblast osteocalcin expression and biomineralization. *Mater Sci Eng C Mater Biol Appl* 2013;33:2757–2765.
- Hench LL. Genetic design of bioactive glass. *J Eur Ceram Soc* 2009;29:1257–1265.
- Serra J, Gonzalez P, Liste S, S. Chiussi, Leon B, Perez-amor M, Ylanen HO, Hupa M. Influence of the non-bridging oxygen groups on the bioactivity of silicate glasses. *J Mater Sci Mater Med* 2002;13:1221–1225.
- Calas G, Cormier L, Galoisy L, Jollivet P. Structure-property relationships in multicomponent oxide glasses. *Comptes Rendus Chemie* 2002;5:831–843.
- Wren AW, Laffir FR, Kidari A, Towler MR. The structural role of titanium in Ca-Sr-Zn-Si/Ti glasses for medical applications. *J Non-Cryst Solids* 2011;357:1021–1026.
- Takadama H, Kim H-M, Kokubo T, Nakamura T. XPS study of the process of apatite formation on bioactive Ti-6Al-4V alloy in simulated body fluid. *Sci Technol Adv Mater* 2001;2:389–396.
- González JEG, Mirza-Rosca JC. Study of the corrosion behaviour of titanium and some of its alloys for biomedical and dental implant applications. *J Electroanal Chem* 1999;471:109–115.
- Lausmaa J. Surface spectroscopic characterization of titanium implant materials. *J Electron Spectroscop* 1996;81:343–361.
- Piscanec S, Ciacchi LC, Vesselli E, Comelli G, Sbaizero O, Meriani S, De Vita A. Bioactivity of TiN-coated titanium implants. *Acta Mater* 2004;52:1237–1245.
- Iwamoto N, Tsunawaki Y, Masao F, Hatfori T. Raman spectra of K₂O-SiO₂ and K₂O-SiO₂-TiO₂ glasses. *J Non-Cryst Solids* 1975;18:303–306.
- Kusaeiraki K. Infrared and Raman spectra of vitreous silica and sodium silicates containing titanium. *J Non-Cryst Solids* 1987;95–96:411–418.
- Satyanarayana T, Kityk IV, Ozga K, Piasecki M, Bragiel P, Brik MG, Ravi Kumar V, Reshak AH, Veeraiyah N. Role of titanium valence states in optical and electronic features of PbO-Sb₂O₃-B₂O₃-TiO₂ glass alloys. *J Alloy Comp* 2009;482:283–297.
- Lakhkar NJ, Lee I-H, Kim H-W, Salih V, Wall B, Knowles JC. Bone formation controlled by biologically relevant inorganic ions: Role and controlled delivery from phosphate-based glasses. *Adv Drug Deliv Rev* 2013;65:405–420.
- Wang JY, Wicklund BH, Gustilo RB, Tsukayama DT. Titanium, chromium and cobalt ions modulate the release of bone-associated cytokines by human monocytes/macrophages *in vitro*. *Biomaterials* 1996;17:2233–2240.
- Liu HC, Chang WH, Lin FH, Lu KH, Tsuang YH, Sun JS. Cytokine and prostaglandin E₂ release from leukocytes in response to metal ions derived from different prosthetic materials: An *in vitro* study. *Artif Organs* 1999;23:1099–1106.
- Chan EP, Mhawi A, Clode P, Saunders M, Filgueira L. Effects of titanium(IV) ions on human monocyte-derived dendritic cells. *Metallomics* 2009;1:166–174.
- Sun ZL, Wataha JC, and Hanks CT. Effects of metal ions on osteoblast-like cell metabolism and differentiation. *J Biomed Mater Res* 1997;34:29–37.
- Liao HH, Wurtz T, Li JG. Influence of titanium ion on mineral formation and properties of osteoid nodules in rat calvaria cultures. *J Biomed Mater Res* 1999;47:220–227.
- Mine Y, Makihiro S, Nikawa H, Murata H, Hosokawa R, Hiyama A, Mimura S. Impact of titanium ions on osteoblast-

- osteoclast- and gingival epithelial-like cells. *J Prosthodont Res* 2010;54:1–6.
35. Murphy S, Wren AW, Towler MR, Boyd D. The effect of ionic dissolution products of Ca–Sr–Na–Zn–Si bioactive glass on in vitro cytocompatibility. *J Mater Sci Mater Med* 2010;10:2827–2834.
36. Talo F, Senila M, Frentiu T, Simon S. Effect of titanium ions on the ion release rate and uptake at the interface of silica based xerogels with simulated body fluid. *Corros Sci* 2013;72:41–46.
37. Abou Neel EA, Chrzanowski W, Knowles JC. Effect of increasing titanium dioxide content on bulk and surface properties of phosphate-based glasses. *Acta Biomater* 2008;4:523–534.
38. Lakhkar N, Abou Neel EA, Salih V, Knowles JC. Titanium and strontium-doped phosphate glasses as vehicles for strontium ion delivery to cells. *J Biomat Appl* 2011;25:877–893.